

MTL TR 90-10

AD

AD-A220 849

SOL-GEL PROCESSING AND CRYSTALLIZATION OF YTTRIUM ALUMINOSILICATES

JAMES C. WALCK

U.S. ARMY MATERIALS TECHNOLOGY LABORATORY
CERAMICS RESEARCH BRANCH

CARLO G. PANTANO

PENNSYLVANIA STATE UNIVERSITY
UNIVERSITY PARK, PA

March 1990

Approved for public release; distribution unlimited.

SD DTIC
ELECTE
APR 24 1990
B
D



**US ARMY
LABORATORY COMMAND
MATERIALS TECHNOLOGY LABORATORY**

**U.S. ARMY MATERIALS TECHNOLOGY LABORATORY
Watertown, Massachusetts 02172-0001**

SECURITY CLASSIFICATION OF THIS PAGE (When Data Entered)

SECURITY CLASSIFICATION OF THIS PAGE (When Data Entered)

Block No. 20

ABSTRACT

Glass in the yttria-alumina-silica system was synthesized using sol-gel techniques. Crystallization behavior of the gel and the glass was examined using variable heating rate data obtained by differential thermal analysis (DTA). The reaction rate constants for crystallization followed an Arrhenius temperature dependence, and the activation energies for crystallization were readily determined. Surface nucleation/crystallization dominated but no appreciable difference in crystallization between the gel and glass powders was evident. In this system it was verified that densification of the gel occurred before the onset of crystallization. Isothermal heat treatment of the gels and glasses produced $3\text{Al}_2\text{O}_3 \cdot 2\text{SiO}_2$ and various polymorphs of $\text{Y}_2\text{O}_3 \cdot 2\text{SiO}_2$.

CONTENTS

	Page
INTRODUCTION	1
BACKGROUND	1
EXPERIMENTAL PROCEDURE	
Sol/Gel Synthesis	2
Methods of Characterization	3
RESULTS	4
DISCUSSION OF RESULTS	
Crystallization of YAS Gels and Glasses	8
Phase Development During Crystallization	10
SUMMARY	11
REFERENCES	12

Accession For	
NTIS GRA&I	<input checked="" type="checkbox"/>
DTIC TAB	<input type="checkbox"/>
Unannounced	<input type="checkbox"/>
Justification	
By	
Distribution/	
Availability Codes	
Dist	Avail and/or Special
A-1	

INTRODUCTION

Glasses in the yttria-alumina-silica (YAS) system are candidate matrices for SiC reinforced composites because of their high elastic moduli and excellent chemical durability.¹⁻³ Moreover, several compositions offer the potential for controlled crystallization into glass ceramics exhibiting low-thermal expansion and elevated temperature stability.⁴ In order to exploit the properties of these glasses and glass ceramics, improved processing techniques and detailed investigations of their crystallization behavior are required. One area being explored to enhance the processing of ceramics and composites is the use of sol-gel technology. Advantages of sol-gel technology include increased homogeneity and reduced processing temperatures. This report focuses on the preparation of YAS gels and the feasibility of obtaining dense glasses and glass-ceramics from them. Of particular interest is the ability to complete the gel-to-glass conversion before the onset of crystallization. Recent observations suggest that gels and gel-derived glasses have higher nucleation rates and lower crystallization temperatures relative to conventionally prepared glasses. This behavior appears to be dominant for compositions which correspond to compounds and/or have strong tendencies for homogeneous nucleation.⁵⁻⁷ A high water content and a large surface area due to internal porosity have been presented as possible reasons for the enhanced crystallization in gels.^{8,9} The objectives of this work were to synthesize $Y_2O_3 \cdot SiO_2$ and ternary YAS gels and glasses, and then use differential thermal analysis and x-ray diffraction to examine the kinetics and phase developments during crystallization.

BACKGROUND

In this report, the crystallization kinetics of gels and glasses are examined by differential thermal analysis (DTA). The use of DTA to evaluate the kinetics of crystallization deserves comment, however, because of uncertainties in the analytical models used to describe crystallization under nonisothermal conditions.¹⁰⁻¹²

The foundation for the model used in this investigation comes from the Johnson-Mehl-Avrami (JMA) equation:

$$x = 1 - \exp[-(Kt)^n] \quad (1)$$

for isothermal solid-state phase transformation kinetics¹³ where x is the volume fraction crystallized, K is the reaction rate constant, t is time, and n is the Avrami exponent. The Avrami exponent depends upon the morphology of crystal nucleation/growth where $n = 1-2$ for surface crystallization and $n = 3-4$ for bulk crystallization. The reaction rate constant is usually assigned an Arrhenius dependence:

$$K = \nu \exp(-E/RT) \quad (2)$$

where ν is the frequency factor and E is the activation energy for the overall crystallization process. K is determined by the nucleation rate (I) and the growth rate (u). Equation 2, therefore, necessarily assumes Arrhenius behavior of both I and u .

Yinnon and Uhlmann reviewed various models derived from the JMA equation for use under nonisothermal conditions and pointed out that most models did not take into account the proper temperature dependence of the reaction rate constant;¹¹ the only exception was the model proposed by Augis and Bennett.¹⁴ Bansal and Doremus¹⁵ used an approach similar

to that of Augis and Bennett to address the temperature dependence of K in terms of heating rate and the exotherm peak temperature, and derived the relation:

$$\ln(T_p^2/\phi) = \ln(E/R) - \ln\nu + (E/RT_p) \quad (3)$$

where T_p is the temperature at the peak of the crystallization exotherm, ϕ is the experimental heating rate, E is the activation energy for the crystallization process, R is the universal gas constant, and ν is a frequency factor. For narrow ranges of temperature, such as those occurring in DSC/DTA experiments where only the exothermic peak is being used for analysis, Bansal and Doremus found that the values for ν and E calculated from this model were in very good agreement with the same parameters calculated from isothermal studies.¹⁶ It should be noted that the Bansal and Doremus model assumes that the exothermic peak, T_p , corresponds to the maximum rate of crystallization for that sample. This is true for DSC, but in DTA, the maximum rate of crystallization typically occurs just prior to T_p .¹⁷ Hammett and Loehman¹⁸ examined the consequences of using DTA results with the Bansal and Doremus model and calculated the activation energy for crystallization of a lithium silicate glass from both DSC and DTA traces. It was found that if a consistent point was chosen to represent a crystallization event from DTA traces, such as the onset temperature or exotherm peak temperature, then activation energies would be obtained which were in very good agreement with those calculated from DSC. For the present work, it is assumed that DTA traces obtained from a variable heating rate technique, used in conjunction with the Bansal and Doremus model, are a reasonable method of calculating the effective activation energy for crystallization.

EXPERIMENTAL PROCEDURE

Sol/Gel Synthesis

The two compositions chosen for examination were 65.0 Y_2O_3 - 35.0 SiO_2 and 42.0 Y_2O_3 - 23.0 Al_2O_3 - 35.0 SiO_2 (in weight percent). In this investigation, yttrium nitrate, yttrium acetate, and yttrium isopropoxide were evaluated as candidate Y^{3+} sources. Aluminum sec-butoxide and distilled TEOS were used as the network forming cation precursors.

The yttrium-silicate solutions synthesized using yttrium nitrate, $Y(NO_3)_3 \cdot xH_2O$, appeared quite homogeneous and were water clear during preparation and gelation. During drying, however, the gels became opaque with a cream color. The x-ray analysis of gels dried at 120°C revealed the obvious presence of $Y(NO_3)_3$ in various states of hydration. Calcination at 600°C eliminated the detection of any nitrates, but because the resultant material was of dubious homogeneity, the use of yttrium nitrate as a precursor was considered unacceptable.

Yttrium acetate, $Y(OOCCH_3)_3 \cdot xH_2O$, was then tried as a precursor, but its limited solubility (9 g/L) precluded its use for the formation of stable (low water content) sols. Yttrium isopropoxide, $Y[OCH(CH_3)_2]_3$, was also attempted, but this alkoxide proved insoluble in the alcohols and other solvents examined.

The precursor problem was solved through the laboratory synthesis of a soluble yttrium alkoxide. Synthesis of the alkoxide was based on an approach reported for the preparation of dielectric and superconducting ceramics¹⁹ and proved suitable for preparation of a homogeneous gel.

The alkoxide was prepared by mixing yttrium acetate with 2-methoxyethanol ($\text{OCH}_3\text{C}_2\text{H}_5\text{OH}$) and then heating to $>125^\circ\text{C}$ under constant refluxing. After 12 hours the solution turned clear with a slight green/yellow tint. The resultant yttrium methoxyethoxide was quite stable and could be stored for long periods at room temperature.

The formation of an alkoxide solution corresponding to $\text{Y}_2\text{O}_3 \cdot 2\text{SiO}_2$ was first attempted by introducing yttrium methoxyethoxide into partially-hydrolyzed TEOS. These sols were unstable and resulted in a fine white crystalline precipitate with an unidentified x-ray pattern. Numerous adjustments to the processing conditions, such as pH, degree of hydrolysis, temperature of mixing, and order of addition, also proved unsuccessful due to precipitation. The synthesis of this composition was not successfully achieved without precipitation.

In contrast, the ternary eutectic YAS composition was successfully synthesized by controlling the kinetics of hydrolysis and polycondensation reactions between the three precursor alkoxides. Distilled $\text{Si}(\text{OC}_2\text{H}_5)_4$ was first partially hydrolyzed using deionized water, anhydrous ethanol, and concentrated HNO_3 as a catalyst. After stirring for one hour at 60°C , $\text{Al}(\text{OC}_4\text{H}_9)_3$ and isopropanol were introduced. The solution remained water clear with no evidence of either $\text{AlO}(\text{OH})$ or $\text{Al}(\text{OH})_3$ precipitate formation. After continuous stirring for an additional one hour at 60°C , the yttrium alkoxide was poured into this aluminosilicate sol. Refluxing continued for two hours while the YAS sol was slowly cooled to room temperature. Formation of an insoluble alkoxide complex, which had occurred in the $\text{Y}_2\text{O}_3 \cdot 2\text{SiO}_2$ system, was avoided and the resulting YAS sol was clear with a color similar to the yttrium alkoxide. At this point, the only water in the system was that used to partially hydrolyze the TEOS. Water in excess of that required for theoretical hydrolysis and polycondensation (2 mol H_2O :1 mol alkoxide) was mixed with desired amounts of the water-deficient YAS solution. This solution remained transparent throughout gelation and drying with no sign of precipitation. Once gelled and dried through 120°C , the material was heated at $2^\circ\text{C}/\text{min}$ to 600°C to remove residual organics. This material is referred to as gel (or gel powder) throughout the remainder of this report.

Some of the gel powder was then heated at $10^\circ\text{C}/\text{min}$ to 1000°C and held for one hour to complete the gel-to-glass conversion. This material is referred to as gel-derived glass (or glass powder) throughout the remainder of this report. Finally, some of the gel was melted at 1500°C in a platinum crucible and then air quenched. This is referred to as melt-derived glass (or glass powder) throughout this report.

Methods of Characterization

Densities of the YAS gel, gel-derived glass, and melt-derived glass were determined using helium pycnometry on 5 cm^3 of sample. Compositional analyses on representative samples were obtained using borate-fluxed emission spectroscopy, with the reported composition being an average of three runs.

DTA was used to investigate the crystallization behavior of the gels and glasses. Samples of gel and melt-derived glass were first pulverized and screened to $-200 +280$ mesh, then analyzed for specific surface area and residual hydroxyl content using BET and diffuse reflectance IR spectroscopy (DRIFTS), respectively. After these analyses, 70 mg of each of the powders were packed into platinum crucibles and loaded into the DTA unit. Great care was taken to keep the particle size, weight, and packing procedure for each YAS sample the same in order to avoid shifting of exotherm peaks due to heat transfer differences within the

samples. In addition to the gel and glass powder samples, bulk melt-derived glass was also examined in the DTA. This was obtained by melting 70 mg of gel in identical platinum DTA crucibles at 1500°C, then quenching at the same rate used to prepare the melt-derived glass powder. Alpha alumina of the same mesh fraction was used as the standard.

In order to examine differences in crystallization behavior between the YAS gel powder, the melt-derived glass powder, and the melt-derived bulk glass, a variable heating rate method was used. The DTA unit was first calibrated by plotting the observed melting point of gold as a function of each heating rate and comparing these values to the actual melting point. This plot was linear with a maximum deviation of 2.5°C at the highest heating rate. The three types of YAS samples were then run at rates of 2.5°C, 5°C, 10°C, and 20°C/min in flowing air with the exotherm peak temperature being determined by the thermal-analysis software. The exotherm peaks observed for the YAS materials were corrected based on the deviation obtained during the gold calibration, and these corrected temperatures were used in the kinetics analysis.

The thermoanalytical model used to calculate the kinetic parameters for crystallization under nonisothermal conditions is given by Equation 3,

$$\ln(T_p^2/\phi) = \ln(E/R) - \ln\nu + (E/RT_p).$$

A plot of $\ln(T_p^2/\phi)$ versus $1/T_p$ should show an Arrhenius dependence with the slope and intercept being proportional to the activation energy and frequency factor, respectively, for the overall crystallization process.

X-ray diffraction was used to characterize the phase development during crystallization. Samples of the -200 mesh gel, melt-derived glass powder, and chunks of bulk melt-derived glass were placed in platinum pans, heated at 10°C/min in flowing air, then held at temperatures between 1000°C and 1400°C for periods of one hour and five hours, respectively. X-ray diffraction patterns were obtained on pulverized samples using $\text{CuK}\alpha$ radiation and scan rates of 4°C 2 θ /min. Because of inconsistencies in the available x-ray diffraction data for the various $\text{Y}_2\text{O}_3\cdot 2\text{SiO}_2$ phases, standard JCPD files, as well as recently reported x-ray diffraction data,^{20,21} were used to identify the $\text{Y}_2\text{O}_3\cdot 2\text{SiO}_2$ polymorphs present in each sample.

RESULTS

The partially hydrolyzed YAS sols remained stable over a period of several weeks. When the moles water:moles alkoxide was greater than 4:1, the solutions gelled within 24 hours at 25°C and remained clear throughout the aging/drying/calcining processes. Monolithic pieces of dried gel were very difficult to obtain. Although the majority of cast samples cracked into cubes 2 to 4 mm on edge, with the greatest extent of cracking occurring before 120°C, the large pieces present after drying tended to remain intact during further heat treatment.

The compositions and densities of the YAS gel, gel-derived glass, and melt-derived glass appear in Table 1. The total percent oxides analyzed for the gel was slightly less than the other samples due to the presence of residual organics. These organics were essentially removed after the 1000°C heat treatment. Compositional analyses revealed that the desired eutectic composition was obtained in all YAS materials. Densities of both the gel-derived glass and melt-derived glass were in very good agreement with values reported for the same composition processed by conventional melting of oxides.³ X-ray diffraction analysis of the

gels, gel-derived glasses, and melt-derived glasses showed only a broad peak centered around $28.5^\circ 2\theta$. BET surface area for the -200 mesh gel and melt-derived glass powders used in the DTA study appears in Table 2. The gel exhibited significantly greater surface area relative to the ground glass.

Table 1. COMPOSITIONS AND DENSITIES OF YAS GEL AND GLASS

Constituent	Gel*	Gel-Derived [†] Glass	Gel-Derived [‡] Glass	Melt-Derived ^{**} Glass	Target
SiO ₂	30.0	33.9	33.0	33.7 (± 1.0)	33w/o
Al ₂ O ₃	21.7	24.4	25.1	23.3 (± 1.0)	25w/o
Y ₂ O ₃	37.4	41.5	41.8	42.6 (± 1.0)	42w/o
Total	89.1	99.8	99.9	99.6	
Density	1.45	3.36	3.38	3.38	3.38 [°]

* Heated at $2^\circ\text{C}/\text{min}$; held 12 hours at 600°C

[†] Heated at $10^\circ\text{C}/\text{min}$; held 1 hour at 1000°C

[‡] Heated at $20^\circ\text{C}/\text{min}$; to 1100°C ; immediately air quenched

^{**} Heated at $10^\circ\text{C}/\text{min}$; held 1 hour at 1500°C

[°] From Reference 1

Table 2. SPECIFIC SURFACE AREA OF YAS POWDERS (-200 MESH)

Material	Surface Area
YAS Gel	126.95 m ² /gm ($\pm 10\%$)
YAS Melt-Derived Glass	0.82 ($\pm 10\%$)
YAS Gel-Derived Glass*	0.56 ($\pm 10\%$)

*Sample heated at $20^\circ\text{C}/\text{min}$ to 1100°C then immediately air quenched

Figure 1 is a composite plot of the DTA results for all three YAS materials heated at 2.5°C and $20^\circ\text{C}/\text{min}$. A single crystallization event was observed for each YAS material, and x-ray diffraction analysis revealed this to be due to the formation of yttrium disilicate ($\text{Y}_2\text{O}_3 \cdot 2\text{SiO}_2$). No exothermic events corresponding to either the formation of mullite or a pre-mullite aluminosilicate spinel were observed. The gel and melt-derived glass powders exhibited well-defined crystallization exotherms, but the gel had an exotherm maximum consistently lower than the glass; both maxima were within 8°C of each other at all heating rates. The melt-derived bulk glass displayed a much broader exotherm with the maximum shifted 90°C to 130°C higher over the 2.5°C and $20^\circ\text{C}/\text{min}$ runs, respectively. The values of T_g , T_p (maximum in the crystallization exotherm), and T_{melt} for all YAS materials are listed in Table 3 and were obtained from the $10^\circ\text{C}/\text{min}$ DTA traces for comparison with literature data on similar compositions.

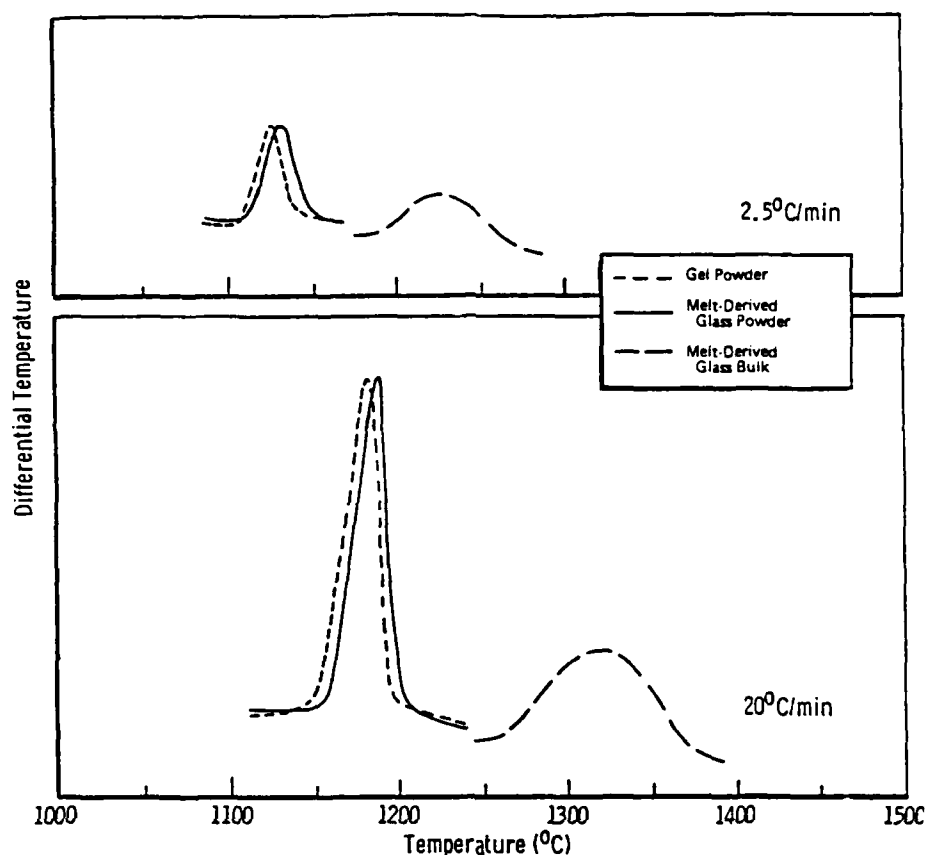


Figure 1. DTA traces for YAS gels and glasses obtained at heating rates of 2.5°C/min and 20°C/min.

Table 3. GLASS TRANSITION, CRYSTALLIZATION PEAK, AND MELTING POINT TEMPERATURES FOR YAS GELS AND GLASSES*

Material	T _g	T _p	T _{melt}
Gel Powder	920	1160	1387
Melt-Derived Glass Powder	918	1165	1386
Melt-Derived Glass Bulk	921	1290	1389
Conventionally Melted Oxides	884 [†] , 925 [‡]	1115 [‡]	1380 ^{**}

*From DTA scans at 10°C/min

†From Reference 3

‡From Reference 37

** From Reference 38

A plot of $\ln(T_p^2/\phi)$ versus $1/T_p$ for the three YAS materials appears in Figure 2. The linearity exhibited in these Arrhenius plots is excellent. The activation energies and frequency factors for crystallization were readily calculated from the linear least-squares fit lines for each set of data in Figure 2, and these values appear in Table 4. The gel powder and

the glass powder had essentially the same activation energy, whereas the bulk glass exhibited an appreciably lower activation energy for crystallization.

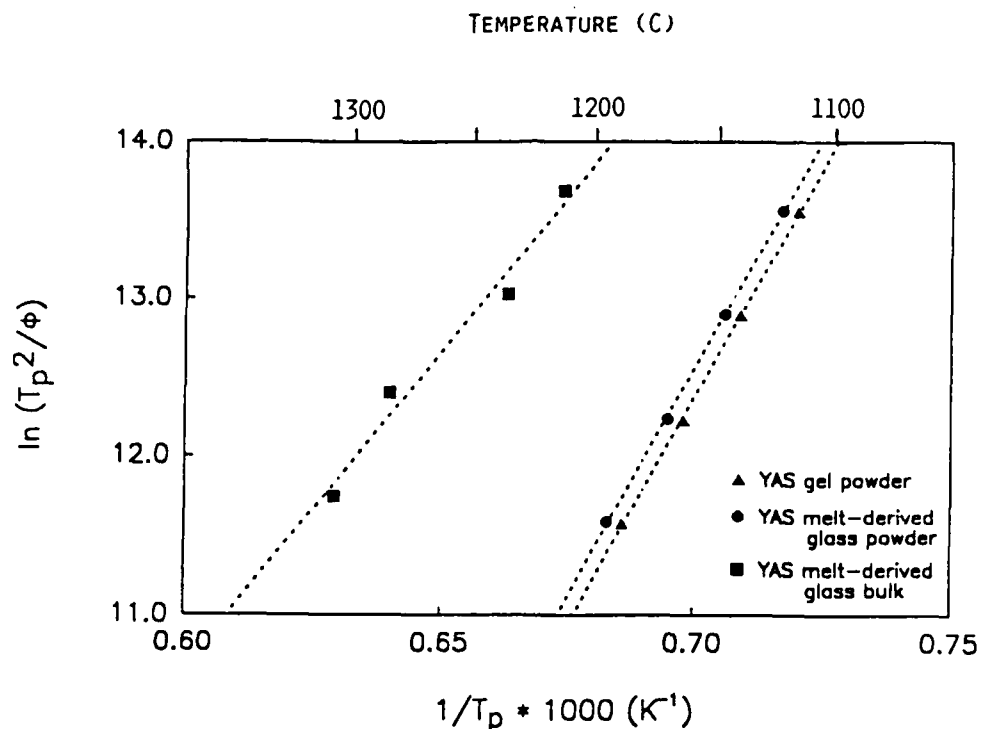


Figure 2. The relationship between exothermic peak temperature, T_p , and heating rate, a , for YAS gels and glasses.

Table 4. KINETIC PARAMETERS OF CRYSTALLIZATION FOR YAS GELS AND GLASSES

	n	E (kJ/mol)	ν (sec ⁻¹)
YAS Gel Powder	1.6	492	1.5×10^{17}
YAS Melt-Derived Glass Powder	1.6	476	1.2×10^{17}
YAS Melt-Derived Glass Bulk	1.7	333	2.2×10^{10}

The crystallization products detected in each YAS sample after isothermal heat treatment for one hour and five hours appear in Table 5. X-ray diffraction analysis showed that all samples remained amorphous up to 1000°C; the gel and glass powders crystallized after treatment at 1100°C, but the bulk glass did not exhibit crystallization until 1200°C. The amorphous peak in the x-ray diffraction patterns shifted from approximately 28.5° in uncrystallized material shown to 26° 2θ as crystallization progressed. Samples held at 1200°C for five hours showed the greatest degree of crystallization. These samples were opaque, white, and remained monolithic during cooling to room temperature. After one hour at 1400°C, all YAS materials melted, but could be cooled to room temperature without crystallization.

Table 5. CRYSTALLIZATION PRODUCTS OF YAS GELS AND GLASSES

	1000°C		1100°C		1200°C		1300°C		1400°C
	1 Hour	5 Hours	1 Hour	5 Hours	1 Hour	5 Hours	1 Hour	5 Hours	1 Hour
YAS Gel and Melt-Derived Glass Powders	A	A	Y	Y M (tr) α (tr)	Y M (tr) α (tr)	Y M α (tr)	β M (tr)	β M	A A
YAS Melt-Derived Glass Bulk	A	A	A	A*	β M (tr)	β M	β M	β M	A

A = Amorphous
 A* = Crystalline scale on sample not detected by xrd
 Y = γ - $\text{Y}_2\text{Si}_2\text{O}_7$
 α = α - $\text{Y}_2\text{Si}_2\text{O}_7$
 β = β - $\text{Y}_2\text{Si}_2\text{O}_7$
 M = Mullite
 (tr) = Trace

DISCUSSION OF RESULTS

Crystallization of YAS Gels and Glasses

Figure 1 shows a substantial decrease in T_p ($\approx 110^\circ\text{C}$) for the glass powder as compared to the bulk glass. This suggests that nucleation and growth from the powder surfaces was responsible for the lower value of T_p . Additional support for a surface crystallization argument comes from the Avrami exponents, which were determined by plotting $\ln(\Delta Y)$ versus $1/T$ where ΔY was the vertical displacement from the baseline at temperature T in each crystallization exotherm.^{16,22} The slope of the linear least-squares fit line for each material equaled $-nE/R$ from Piloyan's relation,²³ and n was calculated using the E values determined for nonisothermal conditions. The n values, which appear in Table 4, are in agreement with a surface nucleation mechanism and imply one-dimensional growth of crystals to the interior of the glass particles from a constant number of surface nuclei.^{24,25}

Figure 2 demonstrates that the reaction rate constant, K , for all YAS materials has an Arrhenius temperature dependence, but that there are differences in the activation energy for crystallization and in the temperature range where the maximum nucleation rate is observed. In the interpretation of these data, it is important to recall that all of the YAS materials were synthesized using organometallic precursors. It can be assumed, therefore, that differences in the impurity levels among the materials are negligible. Further, the bulk glass and the glass powder were both repaired by melting; thus, their thermal history is identical. Finally, the gel powder and glass powder were crushed and sized to equivalent size fractions. These similarities and differences between the various samples are the basis for the discussion that follows.

In the case of the bulk glass, the higher temperature of crystallization and lower activation energy (relative to the powders) suggests that crystallization occurred on preexisting nuclei. It is likely that the glass/Pt cup interface, or the bulk glass surface itself, contained heterogeneous nuclei formed during melting and cooling. The limited surface area of the bulk glass, i.e., relative to the powders, did not allow for any appreciable surface nucleation at lower temperatures. Thus, the observed activation energy probably reflects interfacial rearrangement processes, i.e., rejection of Al and excess Si at the advancing $\text{Y}_2\text{O}_3 \cdot 2\text{SiO}_2$ growth front (see next section).

The glass powder was melted and cooled like the bulk glass, but it possesses a higher, more reactive surface area due to crushing. The lower temperature of crystallization and

higher activation energy (relative to the bulk glass) are consistent with nucleation on particle surfaces and, in this case, the activation energy primarily reflects the barrier to nucleation.

The key issue concerns the gel powder. It was expected that the high internal surface area would lead to an even lower temperature of crystallization than the glass powder. However, it was found that the (microporous) gel powder and (dense) glass powder behaved almost identically. It was hypothesized that the gel-to-glass conversion was complete before the onset of any crystallization. To verify this, YAS gel powder was heated at 20°C/min to 1100°C ($T < T_x$) and then immediately air-cooled. This powder was analyzed and found to be amorphous with a density and specific surface area nearly equal to the melt-derived glass powder (see Table 1). Thus, it could be concluded that the comparable behavior of the gel powders and glass powders in the DTA experiment was due to densification of the gel powder into a gel-derived glass at $T < T_x$. In a more general sense, it revealed that it is possible to sinter YAS gels independent of their crystallization. This behavior is different than that observed for lithium-aluminosilicate (LAS) gels where sintering and crystallization occur simultaneously, and, thereby, limit the densification process.^{26,27}

Finally, the slight shift in the Arrhenius plots between the gel and melt-derived glass powders, corresponding to the observed 8°C to 10°C difference in maximum crystallization rate as shown in Figure 3, should be noted. The effect was found to be due to a higher water content in the sintered gel. Figure 3 compares the IR spectra of the 1100°C sintered gel-derived glass powder and the crushed melt-derived glass powder. The lower hydroxyl content of the melt-derived glass is not surprising since volatilization of residual water could occur more easily during melting than sintering. The lower hydroxyl content of this glass increased its viscosity and, thereby, the temperature where the maximum crystallization rate was observed.

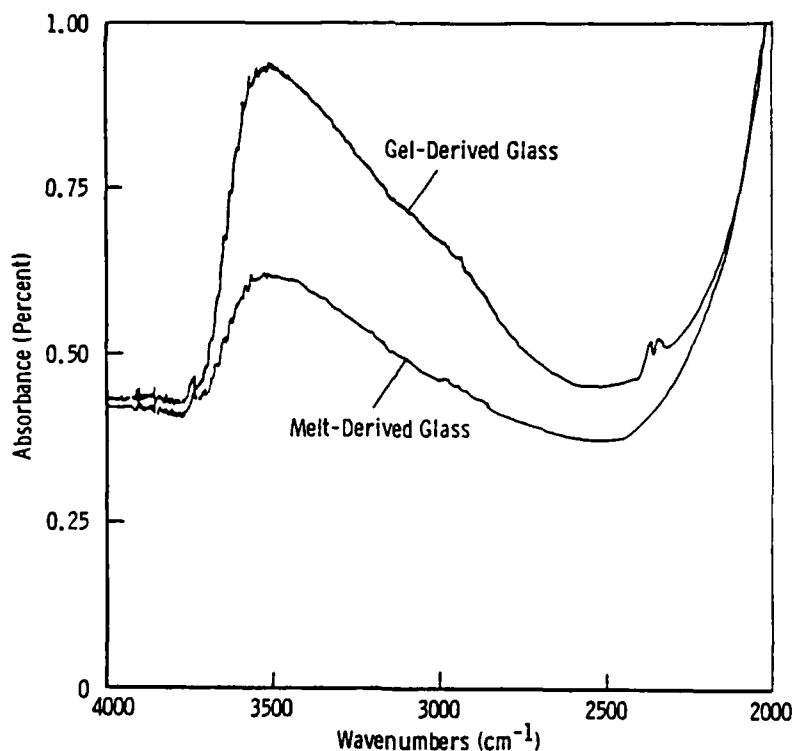


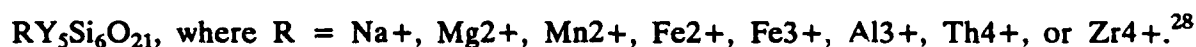
Figure 3. IR spectra showing the relative water content in gel-derived and melt-derived YAS glasses; the broad band at 3500 cm^{-1} is due to both hydroxyl groups and residual water.

Phase Development During Crystallization

The YAS composition studied fell on the tie line between $Y_2O_3 \cdot 2SiO_2$ and $3Al_2O_3 \cdot 2SiO_2$. The gel and glass powders showed development of these phases at $1100^\circ C$, but in the bulk glass, crystallization was not detected until $1200^\circ C$ (see Table 5). Of the five known $Y_2O_3 \cdot 2SiO_2$ polymorphs, three were observed in the crystallized samples.

The initial phase appearing in the gel and glass powders was identified as $\gamma\text{-}Y_2Si_2O_7$. Although uncommon, $\gamma\text{-}Y_2Si_2O_7$ has been observed as the first polymorph during crystallization of yttrium silicate powders²⁸ and YAS grain boundary phases,^{21,29} as well as from oxidation of Y-Al-Si-O-N glasses.^{20,30} A number of x-ray diffraction patterns and crystal structures have been reported for $\gamma\text{-}Y_2Si_2O_7$,^{20,21} but the γ -phase observed in this investigation consistently matched the pattern submitted by Batalieva³¹ for a monoclinic polymorph.

It has been proposed that the formation of $\gamma\text{-}Y_2Si_2O_7$ results from impurity stabilization, and the following formula has been submitted:



Here, the high purity sol-gel precursors should have reduced the chance of multiple impurity influences; if the precipitation of $\gamma\text{-}Y_2Si_2O_7$ requires an impurity cation, it is likely that Al^{3+} is responsible in this case. Recent EDXS analysis has shown a limited solubility of Al^{3+} in $\gamma\text{-}Y_2Si_2O_7$.²¹

The presence of minor amounts of $\alpha\text{-}Y_2Si_2O_7$ in the powders that were heated to $1200^\circ C$ is consistent with the published $\gamma \rightarrow \alpha$ transformation range.²⁸ However, the amount of α -phase after both one and five hours at $1200^\circ C$ remained constant suggesting a limited degree of $\gamma \rightarrow \alpha$ transformation (see Reference 32).

The mixed $\gamma + \alpha$ -phase material completely transformed to $\beta\text{-}Y_2Si_2O_7$ by $1300^\circ C$. The published temperature for the $\alpha \rightarrow \beta$ transformation is $1225 \pm 10^\circ C$.²⁸ It is uncertain whether the γ -phase material first transformed to α before the transformation to β , but for the following reasons, a direct γ to β transformation seems reasonable:

- Both γ and β -phases are monoclinic with very similar unit cell dimensions,
- The α -phase is triclinic with a significant reduction in unit-cell volume, and
- The conversion to $\beta\text{-}Y_2Si_2O_7$ was complete after one hour at $1300^\circ C$.

The YAS bulk melt-derived glass displayed a simplified polymorph development. The initial crystallization product was $\beta\text{-}Y_2Si_2O_7$, and it remained the only polymorph detected prior to the onset of melting. This is in contrast to the powdered glass samples and is consistent with the difference in crystallization kinetics observed in the DTA. Apparently, crystal growth at the high temperatures exhibited in the bulk glass results in the direct precipitation of $\beta\text{-}Y_2Si_2O_7$; this further verifies that nucleation site density plays an important role in the nucleation and stabilization of $Y_2O_3 \cdot 2SiO_2$ polymorphs.

Whereas the immediate development of an yttrium-disilicate phase was always observed, formation of the mullite phase was substantially retarded in all three YAS materials. An amorphous contribution was observed in all x-ray diffraction patterns indicating that none of

the samples were fully crystallized. The shift of this amorphous peak from 28.5° in the uncrystallized material to 26° 2θ in samples exhibiting well-developed $Y_2O_3 \cdot 2SiO_2$, but with little or no mullite, directly reflects a residual aluminosilicate glass. An amorphous hump centered at 26° 2θ has also been reported for mullite glasses³³ and gels,³⁴ and this position corresponds to the most intense diffraction plane for $3Al_2O_3 \cdot 2SiO_2$.

Based on the accounts of phase development in similar rare-earth aluminosilicate glasses, the delayed crystallization of mullite in these YAS glasses is unusual. Both isothermal^{3,28} and nonisothermal³⁵ analyses have shown the immediate development of mullite. The delayed crystallization of mullite in this study is not fully understood since the appropriate $Al_2O_3 \cdot SiO_2$ ratio was present in the system, and the difficulty in retaining mullite glasses (due to rapid devitrification during cooling)^{25,33,36} has been well documented.

SUMMARY

Glass in the yttria-alumina-silica system was successfully synthesized using a sol-gel approach, and the crystallization behavior of the gels and glasses was studied. A variable heating rate DTA method was used to determine the kinetic parameters of crystallization, and isothermal studies were used to characterize phase development. In all materials, the reaction rate constant for the crystallization process followed an Arrhenius temperature dependence. Although surface nucleation/crystallization was found to dominate, no significant difference in the crystallization behavior between microporous gel and dense glass powders was found; therefore, it could be concluded that the gel-to-glass conversion was complete before the onset of crystallization. Isothermal heat treatments produced $Y_2O_3 \cdot 2SiO_2$ and $3Al_2O_3 \cdot 2SiO_2$ crystalline phases; three of the five known yttrium disilicate polymorphs were readily observed (γ , α , and β), but development of the mullite phase was appreciably retarded.

REFERENCES

1. MAKISHIMA, A., TAMURA, Y., and SAKAINO, T. *Elastic Moduli and Refractive Indices of Aluminosilicate Glasses Containing Y_2O_3 , La_2O_3 , and TiO_2* . J. Am. Ceram. Soc., v. 61, no. 5-6, 1978, p. 247-249.
2. MAKISHIMA, A., and SHIMOHARA, T. *Alkaline Durability of High Elastic Modulus Aluminosilicate Glasses Containing Y_2O_3 , La_2O_3 , and TiO_2* . J. Non-Cryst. Solids, v. 38-39, 1980, p. 661-666.
3. HYATT, M., and DAY, D. *Glass Properties in the Yttria-Alumina-Silica System*. J. Am. Ceram. Soc., v. 70, no. 10, ch. 283-287, 1987.
4. APPLEWHITE, A., and DAY, D. *Properties of Y_2O_3 - Al_2O_3 - SiO_2 - M_2O_3 Glasses*. Proceedings of the XVII International Congress on Glass, 1989, p. 337-340.
5. MUKHERJEE, S. *Kinetics of Crystallization of Gels, Gel-Derived Glasses, and Conventional Glasses in the GeO_2 - PbO System*. J. Non-Cryst. Solids, v. 82, 1986, p. 293-300.
6. ZELINSKI, B., FABES, B., and UHLMANN, D. *Crystallization Behavior of Sol-Gel Derived Glasses*. J. Non-Cryst. Solids, v. 82, 1986, p. 307-313.
7. BRANDA, F., ARONNE, A., MAROTTA, M., and BURI, A. *Li_2O - SiO_2 Sol-Gel Glass*. J. Mater. Sci. Lett., v. 6, 1987, p. 203-206.
8. UHLMANN, D., WEINBERG, M., and TEOWEE, G. *Crystallization of Gel-Derived Glasses*. J. Non-Cryst. Solids, v. 100, 1988, p. 154-161.
9. UHLMANN, D., ZELINSKI, B., SILVERMAN, L., WARNER, S., FABES, B., and DOYLE, W. *Kinetic Processes in Sol-Gel Processing*. Science of Ceramic Chemical Processing, Hench and Ulrich, ed., John Wiley & Sons, Inc., New York, 1986, p. 173-183.
10. HENDERSON, D. *Thermal Analysis of Non-Isothermal Crystallization Kinetics in Glass Forming Liquids*. J. Non-Cryst. Solids, v. 30, 1979, p. 301-315.
11. YINNON, H., and UHLMANN, D. *Applications of Thermoanalytical Techniques to the Study of Crystallization Kinetics in Glass-Forming Liquids, Part I: Theory*. J. Non-Cryst. Solids, v. 54, 1983, p. 253-275.
12. SESTAK, J. *A Remark on the Applicability of DTA and the Reliability of Non-Isothermal Determination for the Crystallization Kinetics of Glasses*. J. Thermal Anal., v. 30, 1985, p. 1223-1226.
13. (a) JOHNSON, W., and MEHL, R. *Reaction Kinetics in Processes of Nucleation and Growth*. Trans. Am. Inst. Min., Metal. Pet. Eng., v. 135, 1939, p. 416. (b) AVRAMI, M. *Kinetics of Phase Change: I, General Theory*. J. Chem. Phys., v. 7, no. 12, 1939, p. 1103-1112. (c) AVRAMI, M. *Kinetics of Phase Change: II, Transformation-Time Kinetics for Random Distribution of Nuclei*. J. Chem. Phys., v. 8, no. 2, 1940, p. 212-224. (d) AVRAMI, M. *Kinetics of Phase Change: III, Granulation, Phase Change and Microstructure*. J. Chem. Phys., v. 9, no. 2, 1941, p. 177-184.
14. AUGIS, J., and BENNETT, J. *Calculation of the Avrami Parameters for Heterogeneous Solid State Reactions Using a Modification of the Kissinger Method*. J. Thermal Anal., v. 13, 1978, p. 282-292.
15. BANSAL, N., and DOREMUS, R. *Determination of Reaction Kinetic Parameters From Variable Temperature DSC or DTA*. J. Thermal Anal., v. 29, 1984, p. 115-119.
16. BANSAL, N., DOREMUS, R., and MOYNIHAN, C. *The Crystallization Kinetics of Infrared Transmitting Fluoride Glasses*. Proceedings of the XIV International Congress on Glass, 1986, p. 319-328.
17. WENDLANDT, W. *Thermal Methods of Analysis*, 2nd Ed. John Wiley & Sons, Inc., New York, ch. V, 1974.
18. HAMMETTER, W., and LOEHMAN, R. *Crystallization Kinetics of a Complex Lithium Silicate Glass-Ceramic*. J. Am. Ceram. Soc., v. 70, no. 8, 1987, p. 577-582.
19. RAVINDRANATHAN, P., KOMARNENI, S., BHALLA, A., ROY, R., and CROSS, L. *Sol-Gel Synthesis of Fine-Particle Superconducting Oxide, $YBa_2Cu_3O_{7-x}$* . J. Mater. Res., v. 3, no. 5, 1988, p. 810-812.
20. LIDDELL, K., and THOMPSON, D. *X-ray Diffraction Data for Yttrium Silicates*. Br. Ceram. Trans. J., v. 85, 1986, p. 17-22.
21. DINGER, T., RAI, R., and THOMAS, G. *Crystallization Behavior of a Glass in the Y_2O_3 - SiO_2 - AlN System*. J. Am. Ceram. Soc., v. 71, no. 4, 1988, p. 236-244.
22. KIM, H., RAWLINGS, R., and ROGERS, P. *Sintering and Crystallization Phenomena in the Y_2O_3 - SiO_2 - AlN System*. J. Am. Ceram. Soc., v. 24, 1989, p. 1025-1037.
23. PILOYN, G., RYBACHIKOV, I., and NOVIKOVA, O. *Determination of Activation Energies of Chemical Reactions by Differential Thermal Analysis*. Nature, v. 212, no. 5067, 1966, p. 1229.
24. BANSAL, N., DOREMUS, R., BRUCE, A., and MOYNIHAN, C. *Kinetics of Crystallization of ZrF - BaF - LaF Glass by Differential Scanning Calorimetry*. J. Am. Ceram. Soc., v. 66, no. 4, 1983, p. 233-238.
25. STRAND, Z. *Glass-Ceramic Materials*. Elsevier Applied Science Publishers Co., New York, 1986, p. 63-71.
26. LEE, G. S., Ph.D. Thesis, the Pennsylvania State University, 1989.
27. HAGHIGHAT, R., TREACY, D., PANTANO, C., and KLEIN, L. *Processing and Sintering of Sol-Gel Derived Lithium Aluminosilicate Powders*. Ceram. Eng. Sci. Proc., v. 10, no. 7-8, 1989, p. 707-719.
28. ITO, J., and JOHNSON, H. *Synthesis and Study of Yttrialite*. Amer. Mineral., v. 53, 1968, p. 1940-1952.
29. ALMEIDA, J., FONSECA, A., CORREIA, R., and BAPTISTA, J. *Pressureless Sintering of Silicon Nitride with Additives of the Y_2O_3 - Al_2O_3 - SiO_2 System*. Mater. Sci. Eng., v. A109, 1989, p. 395-400.
30. SMITH, J. *Temperature and Compositional Stability of a $Y_2Si_2O_7$ Phase in Oxidized Si_3N_4* . J. Am. Ceram. Soc., v. 60, no. 9-10, 1977, p. 465-466.
31. BATALIEVA, N., and PYATENKO, I. *Artificial Yttrialite (" γ -Phase") - A Representative of a New Structure Type in the Rare Earth Diorthosilicate Series*. Sov. Phys. Cryst., v. 16, 1972, p. 786-789.
32. DRUMMOND, C., LEE, W., SANDERS, W., and KISER, J. *Crystallization and Characterization of Y_2O_3 - SiO_2 Glasses*. Ceram. Eng. Sci. Proc., v. 9, no. 9-10, 1988, p. 1343-1353.
33. TAKESHI, T., and ROY, R. *Rapid Crystallization of SiO_2 - Al_2O_3 Glasses*. J. Am. Ceram. Soc., v. 56, no. 12, 1973, p. 639-644.
34. SEN, S., and THIAGARAJAN, S. *Phase-Transformations in Amorphous $3Al_2O_3$ - $2SiO_2$ System Prepared by Sol-Gel Method*. Ceramics International, v. 14, 1989, p. 77-86.
35. BEINAROVICH, O., PAVLUSHKIN, N., KHODAKOVSKAYA, Y., and SHALUMOV, B. *Processes of Silicate- and Glass-Formation in a Lanthanum Aluminosilicate Batch Prepared by Codeposition from Solution*. Translated from Fizika i Khimiya Stekla, v. 13, no. 4, 1987, p. 502-509.
36. MORIKAWA, H., MIWA, S., MIYAKE, M., MARUMO, F., and SATA, T. *Structural Analysis of SiO_2 - Al_2O_3 Glasses*. J. Am. Ceram. Soc., v. 65, no. 2, 1982, p. 78-81.
37. DREW, R. *Nitrogen Glass*. P., Evans, ed. Parthenon Press, New York, 1986, p. 50-60.
38. O'MEARA, C., DUNLOP, G., and POMPE, R. *Phase Relations in the System SiO_2 - Y_2O_3 - Al_2O_3* . High Tech. Ceramic, F. Vincenzini, Amsterdam, ed., Elsevier Applied Science Publishers, Co., New York, 1987, p. 265-270.

DISTRIBUTION LIST

No. of Copies	To
1	Office of the Under Secretary of Defense for Research and Engineering, The Pentagon, Washington, DC 20301
	Commander, U.S. Army Laboratory Command, 2800 Powder Mill Road, Adelphi, MD 20783-1145
1	ATTN: AMSLC-IM-TL
1	AMSLC-CT
	Commander, Defense Technical Information Center, Cameron Station, Building 5, 5010 Duke Street, Alexandria, VA 22304-6145
2	ATTN: DTIC-FDAC
1	Metals and Ceramics Information Center, Battelle Columbus Laboratories, 505 King Avenue, Columbus, OH 43201
	Commander, Army Research Office, P.O. Box 12211, Research Triangle Park, NC 27709-2211
1	ATTN: Information Processing Office
	Commander, U.S. Army Materiel Command, 5001 Eisenhower Avenue, Alexandria, VA 22333
1	ATTN: AMCLD
	Commander, U.S. Army Materiel Systems Analysis Activity, Aberdeen Proving Ground, MD 21005
1	ATTN: AMXSY-MP, H. Cohen
	Commander, U.S. Army Missile Command, Redstone Scientific Information Center, Redstone Arsenal, AL 35898-5241
1	ATTN: AMSMI-RD-CS-R/Doc
1	AMSMI-RLM
	Commander, U.S. Army Armament, Munitions and Chemical Command, Dover, NJ 07801
2	ATTN: Technical Library
1	AMDAR-LCA, Mr. Harry E. Peibly, Jr., PLASTEC, Director
	Commander, U.S. Army Natick Research, Development and Engineering Center, Natick, MA 01760
1	ATTN: Technical Library
	Commander, U.S. Army Satellite Communications Agency, Fort Monmouth, NJ 07703
1	ATTN: Technical Document Center
	Commander, U.S. Army Tank-Automotive Command, Warren, MI 48397-5000
1	ATTN: AMSTA-ZSK
2	AMSTA-TSL, Technical Library
	Commander, White Sands Missile Range, NM 88002
1	ATTN: STEWS-WS-VT
	President, Airborne, Electronics and Special Warfare Board, Fort Bragg, NC 28307
1	ATTN: Library
	Director, U.S. Army Ballistic Research Laboratory, Aberdeen Proving Ground, MD 21005
1	ATTN: SLCBR-TSB-S (STINFO)
	Commander, Dugway Proving Ground, Dugway, UT 84022
1	ATTN: Technical Library, Technical Information Division
	Commander, Harry Diamond Laboratories, 2800 Powder Mill Road, Adelphi, MD 20783
1	ATTN: Technical Information Office
	Director, Benet Weapons Laboratory, LCWSL, USA AMCCOM, Watervliet, NY 12189
1	ATTN: AMSMC-LCB-TL
1	AMSMC-LCB-R
1	AMSMC-LCB-RM
1	AMSMC-LCB-RP
	Commander, U.S. Army Foreign Science and Technology Center, 220 7th Street, N.E., Charlottesville, VA 22901-5396
3	ATTN: AIFRTC, Applied Technologies Branch, Gerald Schlesinger

No. of Copies	To
1	Commander, U.S. Army Aeromedical Research Unit, P.O. Box 577, Fort Rucker, AL 36360 ATTN: Technical Library
1	Commander, U.S. Army Aviation Systems Command, Aviation Research and Technology Activity, Aviation Applied Technology Directorate, Fort Eustis, VA 23604-5577 ATTN: SAVDL-E-MOS
1	U.S. Army Aviation Training Library, Fort Rucker, AL 36360 ATTN: Building 5906-5907
1	Commander, U.S. Army Agency for Aviation Safety, Fort Rucker, AL 36362 ATTN: Technical Library
1	Commander, USACDC Air Defense Agency, Fort Bliss, TX 79916 ATTN: Technical Library
1	Commander, U.S. Army Engineer School, Fort Belvoir, VA 22060 ATTN: Library
1	Commander, U.S. Army Engineer Waterways Experiment Station, P. O. Box 631, Vicksburg, MS 39180 ATTN: Research Center Library
1	Commandant, U.S. Army Quartermaster School, Fort Lee, VA 23801 ATTN: Quartermaster School Library
1	Naval Research Laboratory, Washington, DC 20375 ATTN: Code 5830
2	Dr. G. R. Yoder - Code 6384
1	Chief of Naval Research, Arlington, VA 22217 ATTN: Code 471
1	Edward J. Morrissey, WRDC/MLTE, Wright-Patterson Air Force, Base, OH 45433-6523
1	Commander, U.S. Air Force Wright Research & Development Center, Wright-Patterson Air Force Base, OH 45433-6523 ATTN: WRDC/MLC
1	WRDC/MLLP, M. Forney, Jr.
1	WRDC/MLBC, Mr. Stanley Schulman
1	National Aeronautics and Space Administration, Marshall Space Flight Center, Huntsville, AL 35812 ATTN: R. J. Schwinghammer, EH01, Dir, M&P Lab
1	Mr. W. A. Wilson, EH41, Bldg. 4612
1	U.S. Department of Commerce, National Institute of Standards and Technology, Gaithersburg, MD 20899 ATTN: Stephen M. Hsu, Chief, Ceramics Division, Institute for Materials Science and Engineering
1	Committee on Marine Structures, Marine Board, National Research Council, 2101 Constitution Ave., N.W., Washington, DC 20418
1	Librarian, Materials Sciences Corporation, Guynedd Plaza 11, Bethlehem Pike, Spring House, PA 19477
1	The Charles Stark Draper Laboratory, 68 Albany Street, Cambridge, MA 02139
1	Wyman-Gordon Company, Worcester, MA 01601 ATTN: Technical Library
1	Lockheed-Georgia Company, 86 South Cobb Drive, Marietta, GA 30063 ATTN: Materials and Processes Engineering Dept. 71-11, Zone 54
1	General Dynamics, Convair Aerospace Division, P.O. Box 748, Fort Worth, TX 76101 ATTN: Mfg. Engineering Technical Library
1	Mechanical Properties Data Center, Belfour Stulen Inc., 13917 W. Bay Shore Drive, Traverse City, MI 49684
2	Director, U.S. Army Materials Technology Laboratory, Watertown, MA 02172-0001 ATTN: SLCMT-TML
2	Authors

U.S. Army Materials Technology Laboratory
Watertown, Massachusetts 02172-0001
SOL-GEL PROCESSING AND
CRYSTALLIZATION OF YTTRIUM
ALUMINOSILICATES - James C. Walck and
Carlo G. Pantano

Technical Report MTL TR 80-10, March 1980, 15 pp-
illus-tables

AD UNCLASSIFIED
UNLIMITED DISTRIBUTION

Key Words

Sol-gel
Crystallization
Differential thermal analysis

Glass in the yttria-alumina-silica system was synthesized using sol-gel techniques. Crystallization behavior of the gel and the glass was examined using variable heating rate data obtained by differential thermal analysis (DTA). The reaction rate constants for crystallization followed an Arrhenius temperature dependence, and the activation energies for crystallization were readily determined. Surface nucleation/crystallization dominated but no appreciable difference in crystallization between the gel and glass powders was evident. In this system it was verified that densification of the gel occurred before the onset of crystallization. Isothermal heat treatment of the gels and glasses produced $3Al_2O_3 \cdot 2SiO_2$ and various polymorphs of $Y_2O_3 \cdot 2SiO_2$.

U.S. Army Materials Technology Laboratory
Watertown, Massachusetts 02172-0001
SOL-GEL PROCESSING AND
CRYSTALLIZATION OF YTTRIUM
ALUMINOSILICATES - James C. Walck and
Carlo G. Pantano

Technical Report MTL TR 80-10, March 1980, 15 pp-
illus-tables

AD UNCLASSIFIED
UNLIMITED DISTRIBUTION

Key Words

Sol-gel
Crystallization
Differential thermal analysis

Glass in the yttria-alumina-silica system was synthesized using sol-gel techniques. Crystallization behavior of the gel and the glass was examined using variable heating rate data obtained by differential thermal analysis (DTA). The reaction rate constants for crystallization followed an Arrhenius temperature dependence, and the activation energies for crystallization were readily determined. Surface nucleation/crystallization dominated but no appreciable difference in crystallization between the gel and glass powders was evident. In this system it was verified that densification of the gel occurred before the onset of crystallization. Isothermal heat treatment of the gels and glasses produced $3Al_2O_3 \cdot 2SiO_2$ and various polymorphs of $Y_2O_3 \cdot 2SiO_2$.

U.S. Army Materials Technology Laboratory
Watertown, Massachusetts 02172-0001
SOL-GEL PROCESSING AND
CRYSTALLIZATION OF YTTRIUM
ALUMINOSILICATES - James C. Walck and
Carlo G. Pantano

Technical Report MTL TR 80-10, March 1980, 15 pp-
illus-tables

AD UNCLASSIFIED
UNLIMITED DISTRIBUTION

Key Words

Sol-gel
Crystallization
Differential thermal analysis

Glass in the yttria-alumina-silica system was synthesized using sol-gel techniques. Crystallization behavior of the gel and the glass was examined using variable heating rate data obtained by differential thermal analysis (DTA). The reaction rate constants for crystallization followed an Arrhenius temperature dependence, and the activation energies for crystallization were readily determined. Surface nucleation/crystallization dominated but no appreciable difference in crystallization between the gel and glass powders was evident. In this system it was verified that densification of the gel occurred before the onset of crystallization. Isothermal heat treatment of the gels and glasses produced $3Al_2O_3 \cdot 2SiO_2$ and various polymorphs of $Y_2O_3 \cdot 2SiO_2$.

U.S. Army Materials Technology Laboratory
Watertown, Massachusetts 02172-0001
SOL-GEL PROCESSING AND
CRYSTALLIZATION OF YTTRIUM
ALUMINOSILICATES - James C. Walck and
Carlo G. Pantano

Technical Report MTL TR 80-10, March 1980, 15 pp-
illus-tables

AD UNCLASSIFIED
UNLIMITED DISTRIBUTION

Key Words

Sol-gel
Crystallization
Differential thermal analysis

Glass in the yttria-alumina-silica system was synthesized using sol-gel techniques. Crystallization behavior of the gel and the glass was examined using variable heating rate data obtained by differential thermal analysis (DTA). The reaction rate constants for crystallization followed an Arrhenius temperature dependence, and the activation energies for crystallization were readily determined. Surface nucleation/crystallization dominated but no appreciable difference in crystallization between the gel and glass powders was evident. In this system it was verified that densification of the gel occurred before the onset of crystallization. Isothermal heat treatment of the gels and glasses produced $3Al_2O_3 \cdot 2SiO_2$ and various polymorphs of $Y_2O_3 \cdot 2SiO_2$.